PHENOTYPICAL ANALYSIS IN ZEBRAFISH

Between 30 and 60 injected, anaesthetized embryos (a few drops of 4 mg/ml Tricaine (Sigma, Bornem, Belgium) stock solution in 5 ml embryo water) were analyzed per experiment to identify alterations in thoracic duct (TD), parachordal lymphangioblast (PL) string and secondary sprout development or arteriovenous intersomitic vessel (ISV) distribution, and each experiment was repeated at least three times. Only embryos with normal overall morphology and normal trunk circulation were included. We quantitatively analyzed TD/PL string formation by scoring its presence in 10 consecutive somite segments (from somite 5 to somite 15). Confocal imaging was performed using a Zeiss (Zaventem, Belgium) laser scanning microscope LSM510 and the 488 nm laser emission was supplied by an argon laser.

PHENOTYPICAL ANALYSIS IN TADPOLES

Tadpoles were analyzed using a ZeissSV11 stereomicroscope for blood flow and edema at stage 45 (5 dpf). Intracardial injection of tetramethyl-rhodamine-dextran (TRITC-dextran; molecular weight 2000 kDa) at stage 45 was used to specifically label the lymph vessels as the dye is taken up by and persists for several weeks in lymphatic endothelial cells (LECs) upon extravasation form the blood vessels. GFP^+ blood and GFP^+ $TRITC^+$ lymph vasculature in the trunk region at stage 45-47 was documented with a Zeiss Lumar V.12 fluorescence steromicroscope equipped with an AxioCam MrC5 (Zeiss) digital camera and controlled with AxioVision 4.6 software (Zeiss). In addition, GFP^+ blood vascular endothelial cells (BECs) and GFP^+ $TRITC^+$ LECs were sorted using flow cytometry and synectin mRNA levels were quantified using qRT-PCR (see Table S1 for primer

sequences). Lymphangiography was performed using TRITC-dextran (2000 kDa) on stage 45 tadpoles as described [1].

MORPHOMETRIC ANALYSIS OF PROX-1 STAINING IN TADPOLES

In the ventro-dorsal axis, the Prox-1+ area between the ventral border of the trunk and the dorsal margin of the endoderm was quantified as an index of lymphatic lineage emergence; the Prox-1^+ area between the dorsal margin of the endoderm and the dorsal roof of the neural tube was measured to characterize LEC budding / migration; in the anterio-posterior axis, each region was defined from the location of the rectal diverticle to the tip of the tail. Migration of lymphatic cells was scored, by measuring the maximal distance that Prox1^+ cells migrated from the PCV to the dorsal roof.

WESTERN BLOT

Stage 40 tadpoles were snap-frozen, pulverized and lysed in a buffer containing 20 mM Tris, 0.15 M NaCl, 1% Triton X-100, 10% Glycerol and 5 mM EDTA, supplemented with 4% complete protease inhibitor (Roche, Vilvoorde, Belgium). Western Blot was performed using 10% Nupage Bis-tris minigels (Invitrogen, Merelbeke, Belgium) and a goat anti-human synectin antibody (Abcam, Cambridge, UK).

LUCIFERASE REPORTER ASSAY

A reporter plasmid (pGL4-T7- xSynectin-Luc2) was constructed, consisting of, from 5' to 3', the T7 promotor, a short sequence of the *Xenopus* synectin sequence encompassing the target sequences of both synectin-specific morpholinos (40 nucleotides upstream and 31 nucleotides downstream of the ATG), the luciferase open reading frame and a SV40 poly-adenylation signal. Translation of pGL4-T7-xSynectin-Luc2, using the reticulocyte lysate assay (Promega, Leiden, Netherlands), resulted in the production of a chimeric protein, containing 24 amino acid residues of *Xenopus* synectin and an intact full length luciferase, the activity of which was used as a measure of the translation efficiency.

CELL CULTURE EXPERIMENTS

For the LEC spheroid assay, HDLEC (human dermal LECs) cells were obtained from

Promocell (Heidelberg, Germany) and cultered in endothelial medium provided by the supplier. HDLECs were transfected with human synectin-specific or control siRNA (Invitrogen, Table S1) using Oligofectamine (Invitrogen) according to the manufacturer's protocol, and were allowed to aggregate in round-bottom 96-well plates precoated with 0.8% agarose for 24 hours (3000 cells per spheroid). The spheroids were subsequently embedded in 20% matrigel-containing (BD Biosciences, Erembodegem, Belgium) fibrin gels (3 mg/ml fibrinogen from Calbiochem (Nottingham, UK), 2 U/mL thrombin and 200 µg/mL aprotinin from Sigma) and cultured in the presence or absence of VEGFC (200 ng/ml, delta N and delta C[2] in 1% serum-containing medium for 48 hours. After fixation with 4% paraformaldehyde at room temperature for 1 hour, the spheroids were blocked and permeabilized with PBS containing 0.3% Triton, 5% donkey serum and 0.2% bovine serum albumin (BSA), incubated with anti-human CD31 antibody (DakoCytomation, Helsinki, Finland) overnight at +4 °C, before detection with Alexa-488-conjugated secondary antibody (Molecular Probes, Invitrogen). Images of spheroids were captured with a confocal microscope (Zeiss LSM 510).

For the lymphatic reprogramming assay, H5V murine ECs [3] were grown in standard DMEM medium (Lonza, Invitrogen) supplemented with 10% FBS, 2 mM glutamin, 100 U/ml penicillin, and 0.1 mg/ml streptomycin (Lonza). Sox18 lentivirus preparation was performed as previously described [4]. H5V cells were transfected with mouse synectin-specific or control siRNA (Invitrogen, Table S1) using lipofectamine (Invitrogen) according to the manufacturer's protocol at 12h and 80h post lentivirus transfection. Cells were harvested 7 days after virus transfection and expression of Sox18, Prox-1, Nrp1 and synectin was evaluated by quantitative RT-PCR (see Table S1 for primer sequences).

Variable penetrance of the lymphatic defects upon synectin knockdown

We speculate that the variably penetrant synectin^{KD} phenotype and spectrum of defects is due to a combination of reasons, including the use of a submaximal dose of morpholino (incomplete silencing), technical limitations of injecting an identical dose of morpholino, genetic differences of the morphant embryos analyzed (outbred background), uneven dispersion of morpholinos upon daughter cell division, and variable timing of initiation of lymphatic development (occurring within the range of 30 to 50 hpf [5]). As a result, achieving the necessary degree of silencing below the critical biological threshold at the distinct sprouting locations along the PCV becomes stochastic in such experimental conditions.

Lack of evidence for a role of Vegf in lymphatic development in zebrafish

Although Vegfc is the principal Vegf family member promoting lymphatic development, Vegfa can also modulate lymphangiogenesis [6]. Given that synectin regulates Vegf signaling for arterial morphogenesis [7], we also studied whether silencing of the Vegf co-orthologues (Vegfaa; Vegfab) or Vegf receptors (Kdr; Kdr-like) affected lymphatic development. As reported, silencing of Vegfab or Kdr only minimally affected blood vessel formation [8,9]; lymphatic development was normal in these morphants (not shown). Silencing of Vegfaa or Kdr-like caused prominent defects of primary ISVs at a high morpholino dose, in line with previous findings [9,10], precluding reliable analysis of the formation of the TD. When using lower morpholino doses, TD development still appeared normal in these morphant embryos (not shown). These findings are consistent with previous findings that Kdr-like is present in blood vessels, but absent in the PL cells and TD [5]. Furthermore, formation of secondary sprouts was not affected by silencing of Vegfaa or Vegfab in *PLCg1*^{y10}x*Fli1:eGFP*^{y1} embryos (not shown). Overall, since there is no evidence that Vegf/Vegfr2-signaling regulates lymphatic development in zebrafish, we did not further analyze any possible genetic interaction with synectin.

TABLE S1. Morpholino and primer sequences

ZEBRAFISH AND XENOPUS (X) MORPHOLINO SEQUENCES	
Syn^{ATG1} [11]	5'-CGT CCC AAT CCA AGT GGC ATT TTTG-3'
Syn^{ATG2} [11]	5'-TTC TGC GTC CCA ATC CAA GTG GCAT-3'
Syn^{Ctr} [11]	5'-CcT CCg AAT CCA AGT cGC tTT TTa G-3'
Vegfaa^{ATG} [8]	5'-GTA TCA AAT AAA CAA CCA AGT TCA T-3'
Vegfab^{UTR} [8]	5'-GGA GCA CGC GAA CAG CAA AGT TCA T-3'
Kdr-l^{ATG} [8]	5'-CCG AAT GAT ACT CCG TAT GTC ACT T-3'
Kdr^{splice} [9]	5'-GTT TTC TTG ATC TCA CCT GAA CCC T-3'
Nrp2a^{ATG1} [12]	5'-CCA GAA ATC CAT CTT TCC GAA ATG T-3'
Nrp2b^{ATG1} [12]	5'-AAG ATC CAC AGA GCT TTG CGA ATA A-3'
xSyn^{ATG1}	5'-CTG CGG CCA AGA CCA AGA GGC ATT G-3'
xSyn^{ATG2}	5'-GAA CAG TCC AGT ATC ACT TTC AGG G-3'
Standard control	5'-CCT CTT ACC TCA GTT ACA ATT TAT A-3'
qRT-PCR PRIMERS AND PROBES FOR HUMAN (H), MOUSE (M) AND XENOPUS (X) GENES	
hSynectin	FOR: 5'-GCC TTC ATC AAG CGC ATC A-3' REV: 5'-CCG TTA ATG GCC TCG ATC AT-3' PROBE: 5'-CAG CGT GAT CGA CCA CAT CCA CCT-3'
xSynectin	FOR: 5'- CCC AGT CAT GTG ATT TGT GC -3'(Sybr Green qRT-PCR) REV: 5'- CTG GCA GGC TTT TGTTTCTC-3'
mSynectin	Mm01241790_g1 (Premade Taqman Gene expression assays, Applied Biosystems)
mProx-1	Mm00435969_m1 (Premade Taqman Gene expression assays, Applied Biosystems)
mNrp1	Mm00435372_m1 (Premade Taqman Gene expression assays, Applied Biosystems)
mSox18	Mm00656049_gh (Premade Taqman Gene expression assays, Applied Biosystems)
SYNECTIN AND CONTROL SIRNA	
hSynectin	Stealth RNAi™ siRNA (HSS145785 and HSS173868; Invitrogen)
mSynectin	Stealth RNAi™ siRNA (MSS228768; Invitrogen)
Control siRNA	Stealth RNAi™ siRNA negative control (med and high GC; Invitrogen)
PRIMERS FOR ISH PROBES	
xSynectin	FOR: 5'- TGC TGT CCG TGG ATG TGT AT-3' REV: 5'- TCC ATA CCC AGT TCC ACC AT -3' (962 bp: -192 to +871)

TABLE S2. Analysis of the Vascular Phenotype in Control and synectin^{KD} Zebrafish Embryos

	EMBRYOS WITH INDICATED VASCULAR PHENOTYPES (%)					
Substance injected	**Impaired angioblast migration[a]**	**Thin dorsal aorta**	**Abnormal PCV**	**Arrested ISVs[b]**	**Absent ISVs[c]**	**Number of embryos analyzed**
8 ng Syn^{Ctr}	<1	<1	<1	<1	<1	134
4 ng Syn^{ATG1}	<1	<1	<1	<1	<1	143
6 ng Syn^{ATG1}	<1	<1	<1	4	<1	129
8 ng Syn^{ATG1}	<1	4	<1	7	<1	137

The vascular defects observed are expressed as percentage of affected embryos. [a]: percentage of embryos with angioblasts stalling in the lateral plate mesoderm or at intermediate locations of their lateral-medial trajectory at 24 hpf, when these cells already had reached the midline in control embryos. [b]: percentage of 48 hpf embryos in which > 5 ISVs reached only 50% of their normal dorsal trajectory, arresting at the level of the horizontal myoseptum or the floor plate of the neural tube, and thus failed to establish a continuous DLAV. [c]: percentage of 48 hpf embryos in which > 5 ISVs failed to branch from the dorsal aorta at their designated branch sites. DLAV, dorsal longitudinal anastomosing vessel; ISV, intersomitic vessel; PCV, posterior cardinal vein.

TABLE S3. Analysis of thoracic duct (TD) formation in Control and synectin^{KD} Embryos

	EMBRYOS WITH INDICATED LYMPHATIC PHENOTYPES (%)			
Substance injected	**No TD formation[a]**	**10-30% TD formation [b]**	**30-90% TD formation [c]**	**Number of embryos analyzed[d]**
Buffer	1	1	8	165
9 ng Syn^{Crl}	0	0	9	34
3 ng Syn^{ATG1}	5*	4*	28*	115
6 ng Syn^{ATG1}	13*	10*	37*	112
9 ng Syn^{ATG1}	32*	14*	36*	76
3 ng Syn^{ATG2}	2	7	24	100
4.5 ng Syn^{ATG2}	5*	9*	43*	44
6 ng Syn^{ATG2}	14*	19*	38*	52

[a]: percentage of 7 dpf embryos displaying complete lack of TD formation; [b] percentage of 7 dpf embryos in which the TD formed in only 1-3 out of 10 somites analyzed; [c] percentage of 7 dpf embryos in which the TD formed in 3-9 out of 10 somites analyzed; [d]: number of embryos analyzed in at least 3 experiments. For each condition, the remaining percentage of embryos, display normal TD development. * $P<0.001$ by Chi-square analysis.

TABLE S4. Analysis of Parachordal Lymphangioblast (PL) cells

	EMBRYOS WITH INDICATED LYMPHATIC PHENOTYPES (%)			
Substance injected	**No PL cells[a]**	**10-30% PL cell cord[a]**	**30-90% PL cell cord[a]**	**Number of embryos analyzed[b]**
Buffer	1	0	49	207
8 ng Syn^{Ctr}	0	3	56	39
3 ng Syn^{ATG1}	5*	5*	56*	77
6 ng Syn^{ATG1}	13*	20*	56*	164
9 ng Syn^{ATG1}	28*	27*	40*	105
3 ng Syn^{ATG2}	5	7	29	84
4.5 ng Syn^{ATG2}	22*	36*	25*	36
6 ng Syn^{ATG2}	27*	22*	33*	64

[a]: percentage of 60 hpf embryos lacking PL cells entirely; [b] percentage of 60 hpf embryos displaying PL cells in only 1-3 out of 10 somites; [c] percentage of 60 hpf embryos displaying PL cells in only 1-3 out of 10 somites; [b]: number of embryos analyzed in 3 to 6 experiments; For each condition, the remaining percentage of embryos, display normal PL development; * $P<0.001$ by Chi-square analysis.

TABLE S5. Analysis of the Vascular Phenotypes in Control and synectin^{KD} *Xenopus* Tadpoles

	TADPOLES WITH INDICATED VASCULAR PHENOTYPES (%)				
Substance injected	**Edema[a]**	**Blood flow defects[b]**	**Blood vessel defects[c]**	**DCLV defect**	**Number of tadpoles analyzed**
30 ng xSyn^{Crl}	<1	<1	<1	<1	98
75 ng xSyn^{Crl}	8	10	<1	9	58
15 ng xSyn^{ATG}	9	2	3	16	79
22.5 ng xSyn^{ATG}	15	10	9	38	73
30 ng xSyn^{ATG}	32	25	17	57	107
50 ng xSyn^{ATG2}	42	17	20	65	49
75 ng xSyn^{ATG2}	84	48	22	88	32

The vascular defects observed are expressed as percent of affected embryos. [a]: percentage of tadpoles showing lymphedema in the heart and/or gut region at 5 dpf. [b]: percentage of 5 dpf tadpoles displaying blood circulation defects in the trunk and tail region, as determined by normal light microscopy screening of circulating erythrocytes. [c]: percentage of 5 dpf tadpoles showing (minor) blood vascular defects. In the majority of the affected tadpoles these defects were characterized by a reduced branching of the ISVs. DCLV, Dorsal caudal lymph vessel; ISV, intersomitic vessel.

FIGURE S1. MODEL OF LYMPHATIC DEVELOPMENT IN ZEBRAFISH EMBRYOS

The scheme of lymphatic development (copied from reference [13]) is shown here again for reasons of clarity and to improve understanding of the model. In all panels, a schematic figure is shown on the left, and for panel A,B,D a high-magnification image of the blood and lymphatic vasculature at different stages of development in *Fli1:eGFP*^{y1} zebrafish on the right. For clarity, the confocal images are flanked by redrawings of the vessel contours. DA, dorsal aorta; DLAV, dorsal longitudinal anastomosing vessel; DLLV, dorsal longitudinal lymph vessel; ISV, intersomitic vessel; aISV, arterial ISV; LISV, lymphatic ISV; vISV, venous ISV; PCV, posterial cardinal vein; PL, parachordal lymphangioblast string; TD, thoracic duct. Permanent lymphatic structures (LISV, TD) are labeled dark green; transient lymphangiogenic structures (lymphangiogenic secondary sprouts; PL cells) are labeled light green. **(A-A')** From around 30 hpf onwards, secondary sprouts arise from the PCV. About half of them will give rise to lymphatic structures and are therefore named lymphangiogenic secondary sprout (Ly sec. sprout; yellow arrows in A'). The other half of the secondary sprouts remain venous in nature (angiogenic secondary sprouts) (blue in A). **(B-B')** By 48 hpf, the lymphangiogenic sprouts (yellow arrows in B') radially migrate dorsally to the level of the horizontal myoseptum, where they migrate tangentially to give rise to a transiently existing string of PL cells. The angiogenic sprouts connect to the aISV (red), which thereby will acquire a venous identity. **(C)** Around 60 hpf, PL cells turn and switch from tangential to radial migration closely along aISVs, thereby forming lymphatic intersomitic vessels (LISVs); note the close association of LISVs with aISVs. LISVs that ascend form the dorsal longitudinal lymph vessel (DLLV), while those that descend form the TD. ISVs that connected to the angiogenic secondary sprouts progressively loose their arterial identity and acquire a venous fate. **(D-D')** From 3 days onwards, the first TD fragments appear at distinct locations along the trunk and, via tangential migration, extend rostrally and caudally to merge into a complete TD. The LISV and TD are indicated by white arrows and arrowhead, respectively, in D'.

FIGURE S2. SYNECTIN IS EXPRESSED BY LECS *IN VITRO*

RT-PCR analysis of a panel of human LECs (HMVEC-Lly, human lung LECs; HMVEC-dLyAd and HDLEC, human dermal LECs; hTERT-DHLEC and iLEC, immortalized LECs) and human umbilical vein ECs (HUVEC) cells showed that synectin is expressed in all these cell types *in vitro*. Values represent mRNA levels relative to β-actin.

FIGURE S3. NORMAL VASCULAR MORPHOGENESIS IN SYNECTIN^{KD} ZEBRAFISH EMBRYOS

In all panels, the head faces left and dorsal is up. Scale bars represent 100 µm. DA, dorsal aorta; PAV, parachordal vessel; PCV, posterior cardinal vein; TD, thoracic duct. **(A-B)** Confocal images of the head vasculature of 24 hpf control (A) and synectin^{KD} (B) *Fli1:eGFP^{y1}* zebrafish embryos, showing normal vascular morphogenesis in the morphant embryos. Arow indicates the mid-cerebral vein. **(C-D)** Confocal images of intestinal vessels (arrow) in a 3 dpf control (C) and synectin^{KD} (D) *Fli1:eGFP^{y1}* zebrafish embryo, showing normal morphology, size and branching density of these vessels in the morphant embryo. **(E-F)** Confocal images of the trunk of a 10 dpf control (E) and synectin^{KD} (F) *Fli1:eGFP^{y1}* zebrafish embryo, revealing normal trunk vasculature including the parachordal vessel (PAV). Note the lack of TD in synectin^{KD} embryos (asterisks). Arrows highlight TD in control embryos.

FIGURE S4. ANALYSIS OF TD FORMATION

Figure S4 (copied from reference [13]) is shown here again to clarify the quantification method of the TD formation as an example. DA, dorsal aorta; DLAV, dorsal longitudinal anastomosing vessels; ISV, intersomitic vessel; PCV, posterial cardinal vein; PL, parachordal lymphangioblast string; TD, thoracic duct. TD formation was quantified by measuring the length over which it formed in 10 consecutive somite segments (i.e. somites 5-15; demarcated by the green rectangle). Confocal images of control and morphant *Fli:eGFP^{y1}* embryos are depicted in the insets. Inset A: in the control embryo, a continuous TD formed over all 10 somite segments (100% TD formation; green arrowheads). Inset B:

morphant embryo, in which the TD formed over only 10% (green arrowhead); in the morphant embryo shown, Dll4 expression was silenced [13]. Inset a' and b': schematic redrawing of the DA, TD and PCV in the embryo shown in inset a and b, respectively, with the TD or TD segment marked in green. Scale bars: 200 μm in A-D, 100 μm in E and insets of E.

FIGURE S5. SYNECTIN EXPRESSION IN TADPOLES

Scale bar represents 500 μm in A,B and 250 μm in C-F. In all panels, the dorsal side of the embryo is at the top of the figure and head faces left. G, gut; NT, neural tube; P, pronephric duct; S, somite. Whole-mount *in situ* hybridization of stage 40 *Xenopus* laevis tadpoles using *synectin*-specific antisense (A,C,E) and sense (B,D,F) probes. Synectin was ubiquitously expressed in the NT and S, as well as in the dorsal region, where the longitudinal anastomosing vessels and dorsal caudal lymph vessel (black arrow) form, and in the ventral region, where the PCV and ventral caudal lymph vessel (white arrow) form. Except for the dorsal roof of the NT, no signal was detected with the sense probe.

FIGURE S6. MOPRHOLINO EFFICIENCY OF XSYN^{ATG1} AND XSYN^{ATG2}

(A) To demonstrate the efficacy of xSyn^{ATG1} and xSyn^{ATG2} *in vitro*, we used a previously developed luciferase reporter assay [1]. Briefly, we cloned 80 nucleotides of the *Xenopus* synectin cDNA, including the target sequences of both morpholinos, upstream of and in frame with an open reading frame of the luciferase cDNA (lacking the initiator ATG codon). Expression of this chimeric reporter protein in erythrocyte lysates was monitored via luminometry. Compared to standard control morpholino (SC) (black bar), supplementation of xSyn^{ATG1} (orange bars) or xSyn^{ATG2} (yellow bars) dose-dependently blocked the expression of this chimeric reporter. Error bars represent the SEM. **(B)** To determine whether the amount of synectin protein was reduced in synectin^{KD} tadpoles, we used immunoblot analysis, employing a cross-reacting goat anti-human synectin antibody (*Xenopus* synectin is 74% identitical to human synectin), showing that xSyn^{ATG1} dose-

dependently inhibited translation of synectin *in vivo* (~40 kDa). Densitometry analysis showed that synectin protein levels were reduced by 41% and 66% in synectin^{KD} tadpoles at 30 and 50 ng of xSyn^{ATG1}, respectively. The comparable intensity of the ~55 kDa signal (non-specifically recognized by the goat anti-human synectin antibody) shows equal loading in every lane.

FIGURE S7. LYMPHATIC DEVELOPMENT UPON KNOCKDOWN OF NRP2 IN ZEBRAFISH EMBRYOS

(A) Knockdown of Nrp2b did not disturb TD development (N=64, 16 and 69 for 0, 5 and 10ng of Nrp2b^{ATG}, respectively). **(B)** Quantification of unilateral secondary sprouts in 10 somites of *Fli1:eGFP^{y1}xPLCγ1^{y10}* embryos at 48 hpf revealed that neither single Nrp2a knockdown (up to 10 ng of Nrp2a^{ATG1}; N=48) nor co-knockdown of synectin (2.5 ng Syn^{ATG1}) and Nrp2a (5 ng Nrp2a^{ATG1}) affected secondary sprout formation. (N=50, 6, 10 and 8 for control, single Nrp2a^{L-KD}, Syn^{L-KD} and double morphant embryos). Error bars represent SEM.

REFERENCES

1. Ny A, Koch M, Schneider M, et al. A genetic Xenopus laevis tadpole model to study lymphangiogenesis. *Nat Med*. 2005;11(9):998-1004.
2. Karpanen T, Heckman CA, Keskitalo S, et al. Functional interaction of VEGF-C and VEGF-D with neuropilin receptors. *Faseb J*. 2006;20(9):1462-1472.
3. Garlanda C, Parravicini C, Sironi M, et al. Progressive growth in immunodeficient mice and host cell recruitment by mouse endothelial cells transformed by polyoma middle-sized T antigen: implications for the pathogenesis of opportunistic vascular tumors. *Proc Natl Acad Sci U S A*. 1994;91(15):7291-7295.
4. Francois M, Caprini A, Hosking B, et al. Sox18 induces development of the lymphatic vasculature in mice. *Nature*. 2008;456(7222):643-647.
5. Hogan BM, Bos FL, Bussmann J, et al. ccbe1 is required for embryonic lymphangiogenesis and venous sprouting. *Nat Genet*. 2009;41(4):396-398.
6. Tammela T, Alitalo K. Lymphangiogenesis: Molecular mechanisms and future promise. *Cell*. 2010;140(4):460-476.
7. Lanahan AA, Hermans K, Claes F, et al. VEGF receptor 2 endocytic trafficking regulates arterial morphogenesis. *Dev Cell*. 2010;18(5):713-724.
8. Bahary N, Goishi K, Stuckenholz C, et al. Duplicate VegfA genes and orthologues of the KDR receptor tyrosine kinase family mediate vascular development in the zebrafish. *Blood*. 2007;110(10):3627-3636.
9. Covassin LD, Villefranc JA, Kacergis MC, Weinstein BM, Lawson ND. Distinct genetic interactions between multiple Vegf receptors are required for development of different blood vessel types in zebrafish. *Proc Natl Acad Sci U S A*. 2006;103(17):6554-6559.
10. Nasevicius A, Larson J, Ekker SC. Distinct requirements for zebrafish angiogenesis revealed by a VEGF-A morphant. *Yeast*. 2000;17(4):294-301.
11. Chittenden TW, Claes F, Lanahan AA, et al. Selective regulation of arterial branching morphogenesis by synectin. *Dev Cell*. 2006;10(6):783-795.
12. Yu HH, Moens CB. Semaphorin signaling guides cranial neural crest cell migration in zebrafish. *Dev Biol*. 2005;280(2):373-385.
13. Geudens I, Herpers R, Hermans K, et al. Role of Dll4/Notch in the Formation and Wiring of the Lymphatic Network in Zebra Fish. *Arterioscler Thromb Vasc Biol*. Prepublished on May, 13, 2010, as DOI:10.1161/ATVBAHA.110.203034.

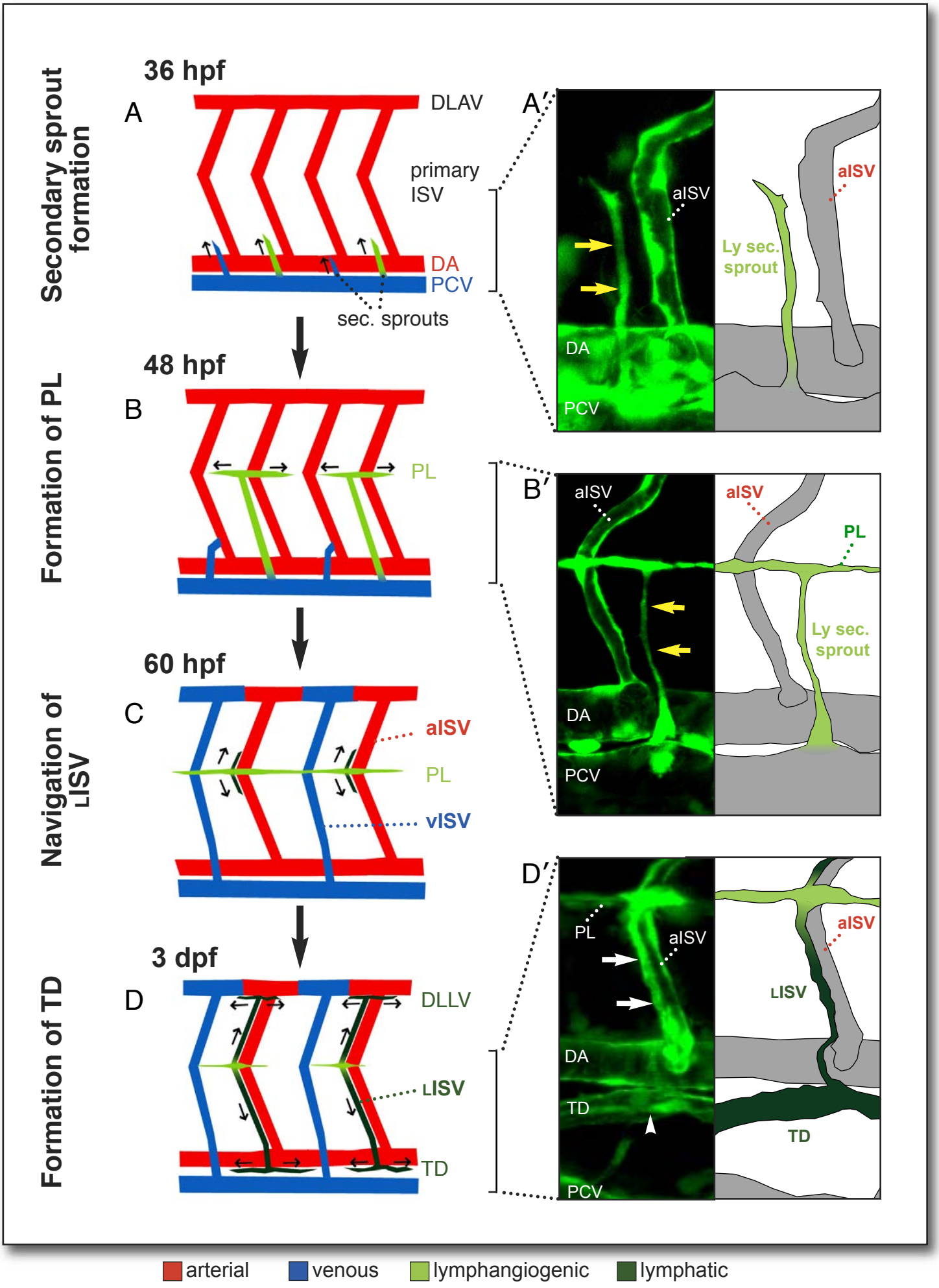
Secondary sprout formation
Formation of PL
Navigation of LISV
Formation of TD
36 hpf
A
DLAV
primary ISV
DA
PCV
sec. sprouts
A′
aISV
Ly sec. sprout
DA
PCV
48 hpf
B
PL
B′
aISV
PL
Ly sec. sprout
60 hpf
C
aISV
PL
vISV
3 dpf
D
DLLV
LISV
TD
D′
PL
LISV
arterial
venous
lymphangiogenic
lymphatic

Figure S1

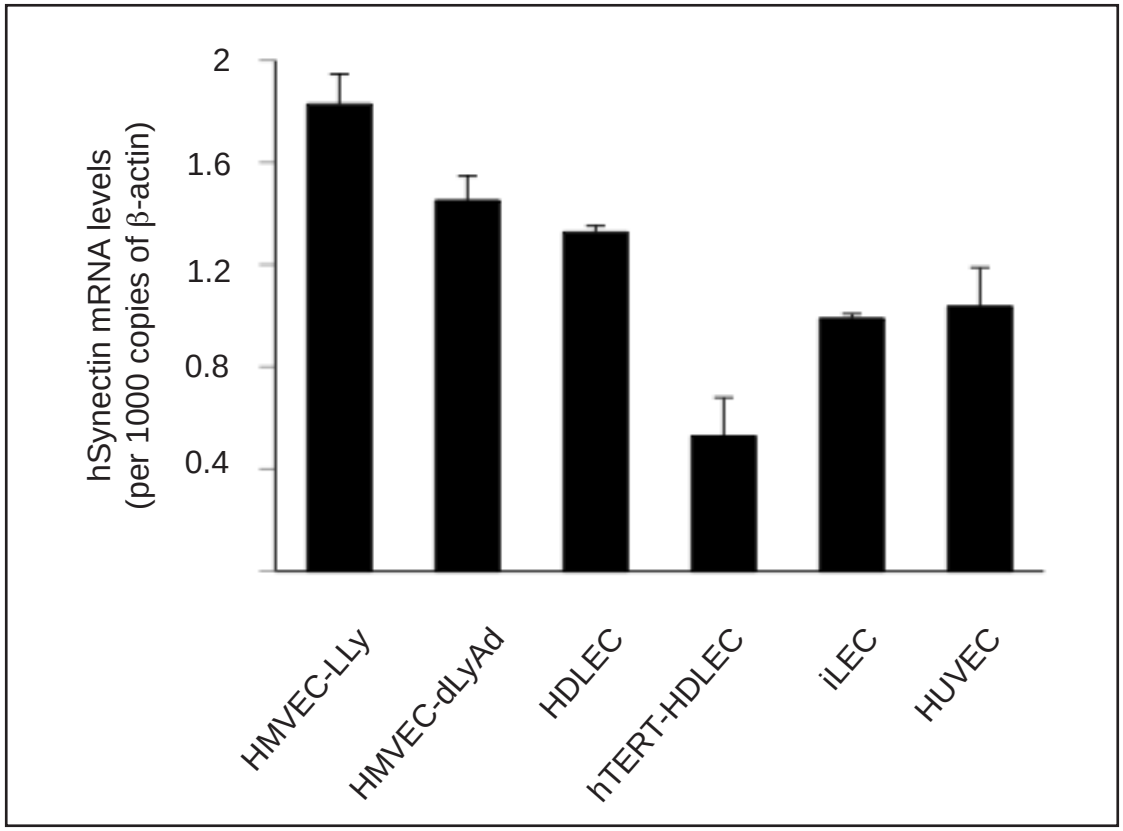
hSynectin mRNA levels
(per 1000 copies of β-actin)
2
1.6
1.2
0.8
0.4
HMVEC-LLy
HMVEC-dLyAd
HDLEC
hTERT-HDLEC
iLEC
HUVEC

Figure S2

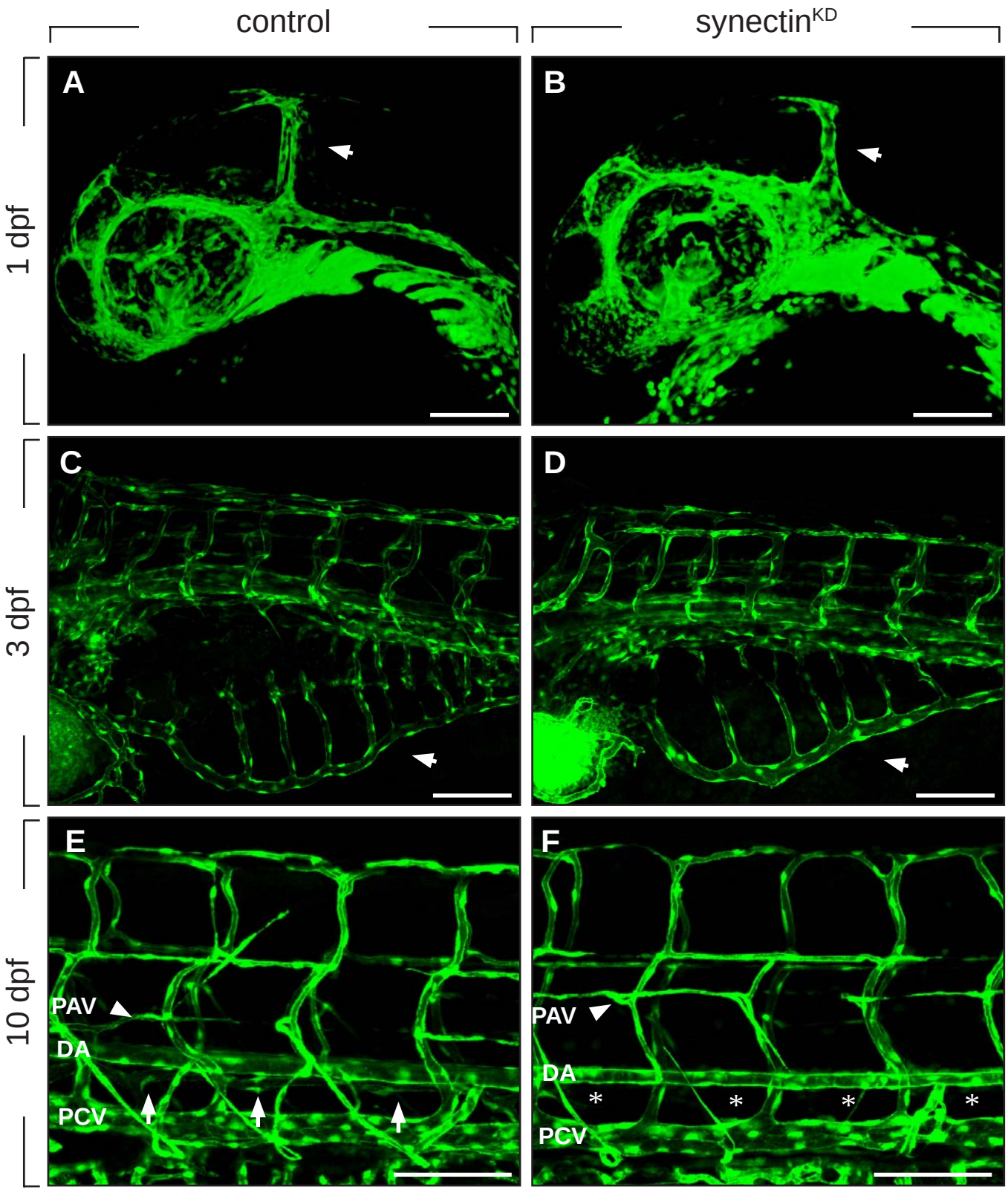
control
synectin^KD
1 dpf
3 dpf
10 dpf
A
B
C
D
E
F
PAV
DA
PCV
PAV
DA
PCV

Figure S3

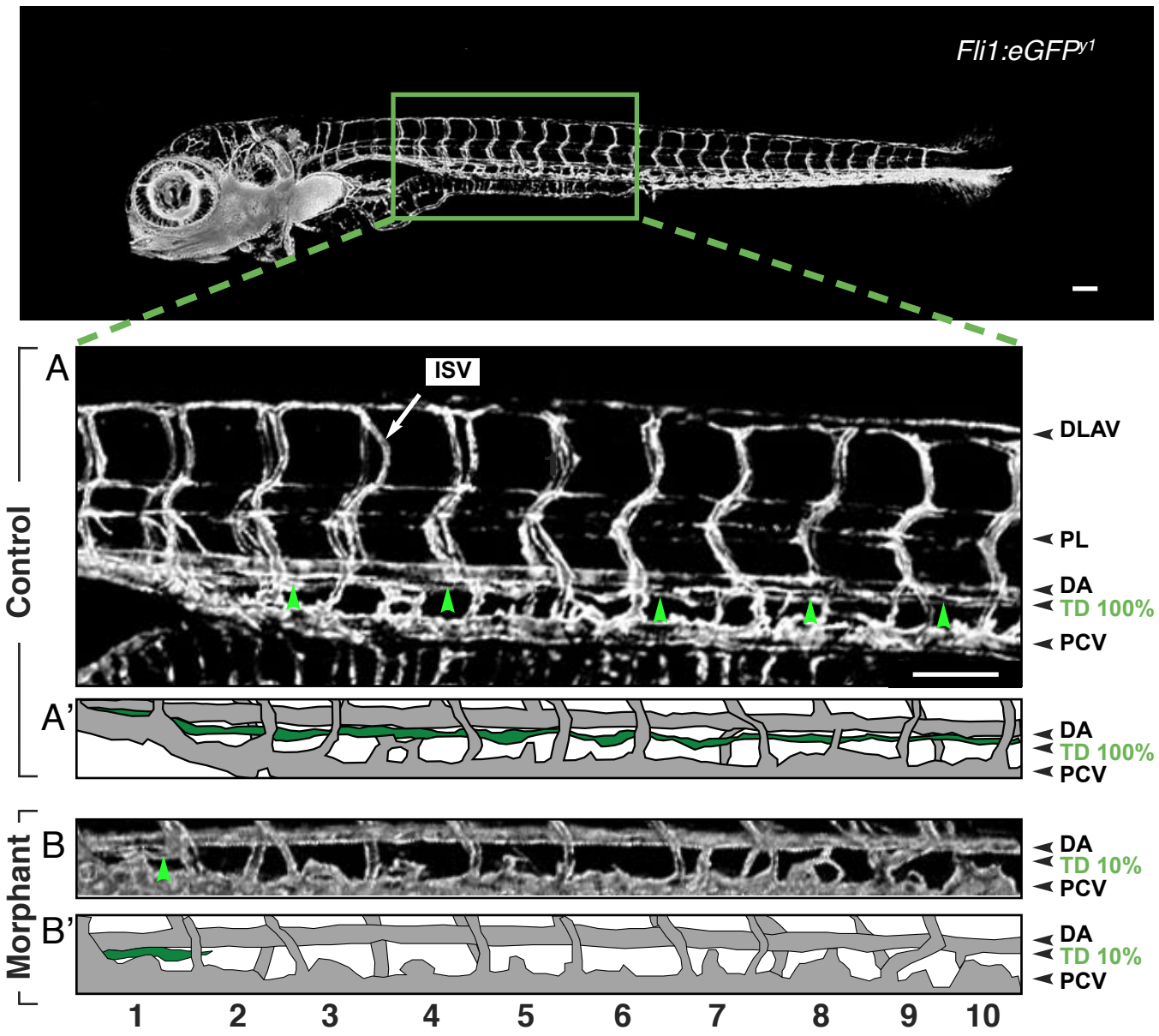
Fli1:eGFP^y1
A
ISV
DLAV
PL
DA
TD 100%
PCV
Control
A'
DA
TD 100%
PCV
B
DA
TD 10%
PCV
Morphant
B'
DA
TD 10%
PCV
1
2
3
4
5
6
7
8
9
10

Figure S4

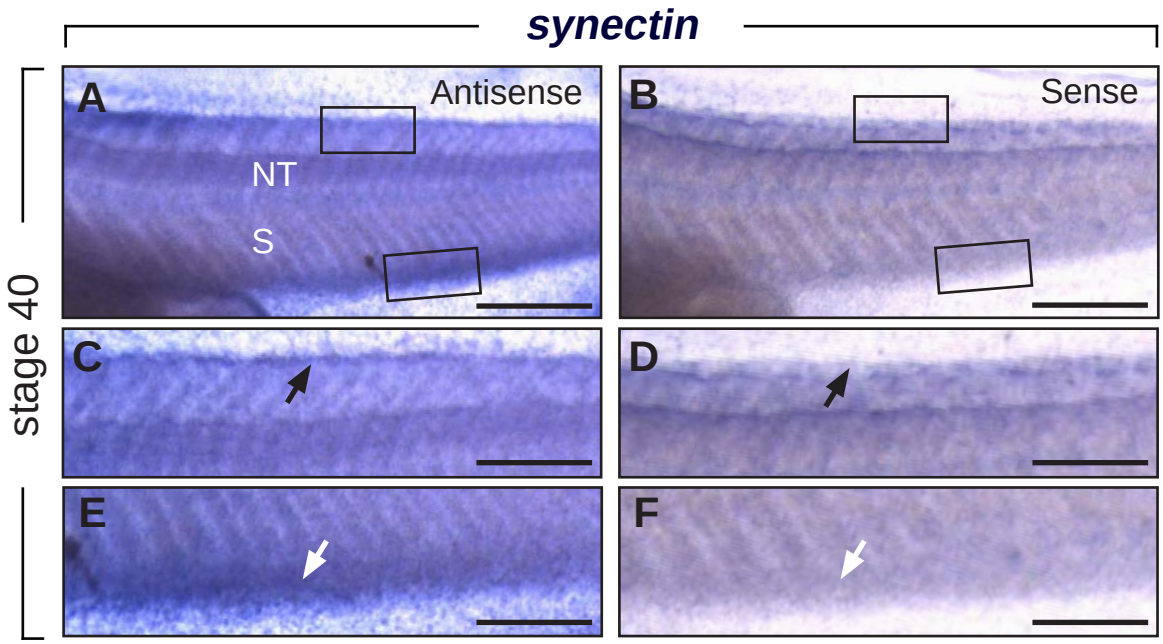

Figure S5

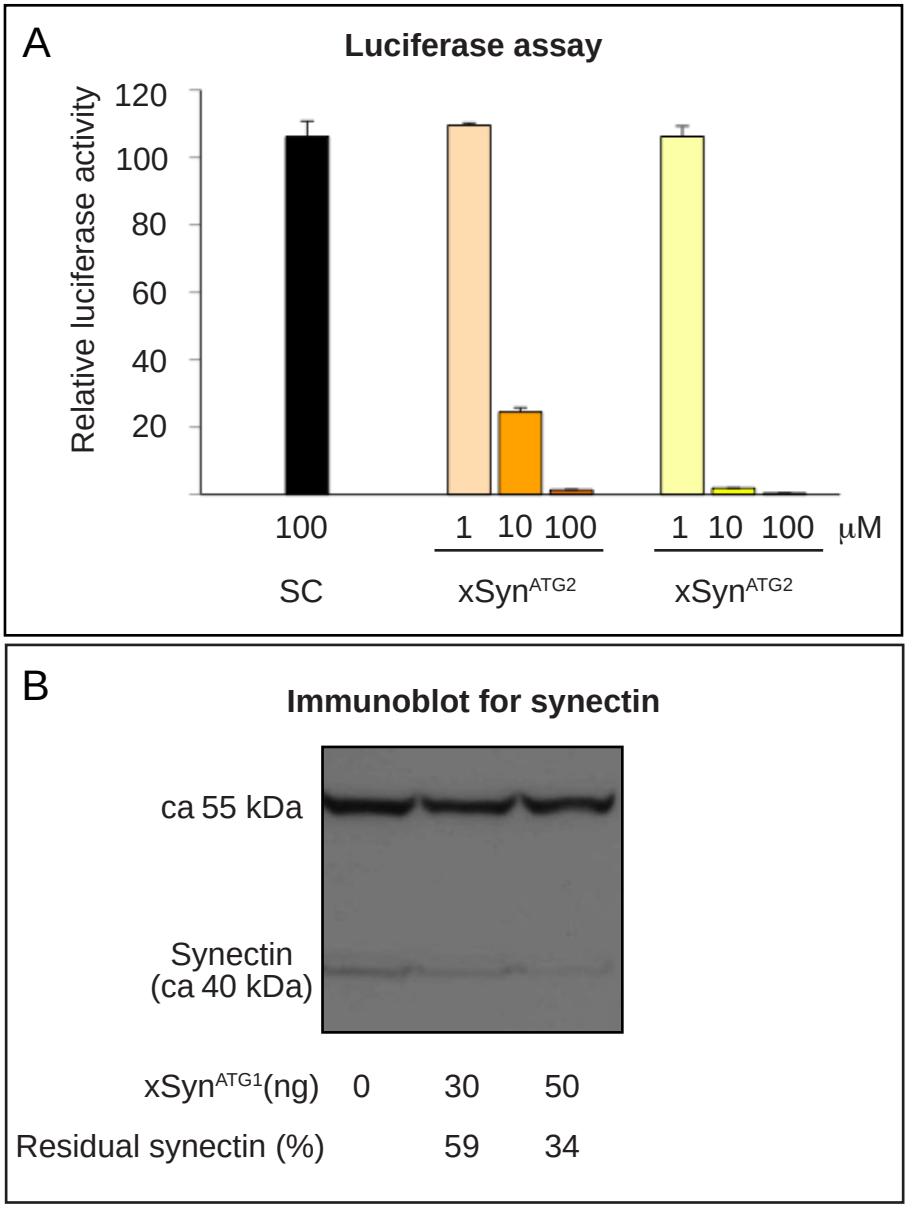
A
Luciferase assay
Relative luciferase activity
120
100
80
60
40
20
100
1 10 100
1 10 100
μM
SC
xSynATG2
xSynATG2
B
Immunoblot for synectin
ca 55 kDa
Synectin
(ca 40 kDa)
xSynATG1(ng) 0 30 50
Residual synectin (%) 59 34

Figure S6

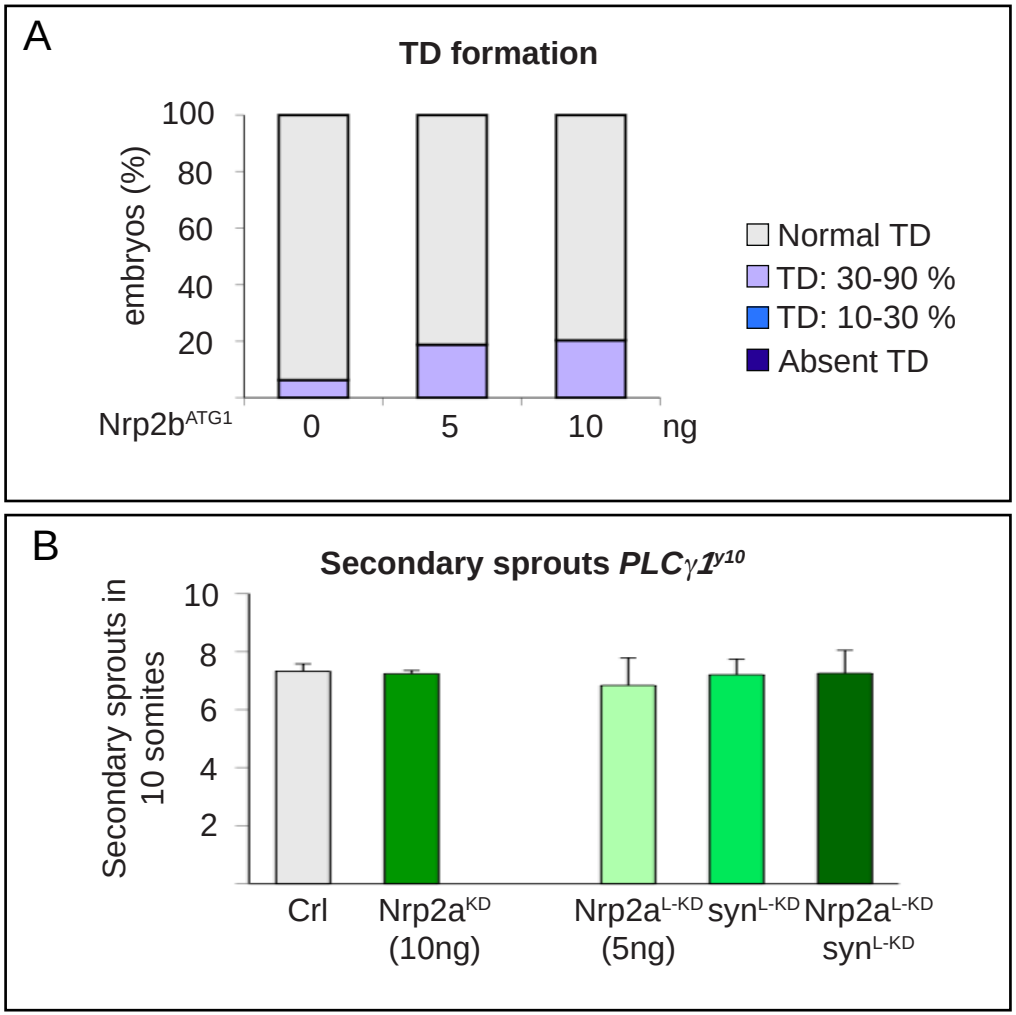
A
TD formation
100
80
60
40
20
embryos (%)
Nrp2b^ATG1
0
5
10
ng
Normal TD
TD: 30-90 %
TD: 10-30 %
Absent TD
B
Secondary sprouts PLCγ1^γ10
Secondary sprouts in 10 somites
10
8
6
4
2
Crl
Nrp2a^KD (10ng)
Nrp2a^L-KD (5ng)
syn^L-KD
Nrp2a^L-KD syn^L-KD

Figure S7